

Structural Condition Assessment of Reinforced Concrete Bridge Using Operational Modal Analysis and Finite Element Model

Hussein Muhammad¹, Sakhiah Abdul Kudus^{1,2*}, Adiza Jamadin^{1,2}, Siti Shahirah Saidin³

¹ School of Civil Engineering, College of Engineering
Universiti Teknologi MARA, 40450 Shah Alam, Selangor, MALAYSIA

² Institute for Infrastructure Engineering and Sustainable Management (IIESM),
Universiti Teknologi MARA (UiTM), Shah Alam, Selangor, MALAYSIA

³ Faculty of Engineering, MAHSA University,
Jalan SP 2, Bandar Saujana Putra, 42610 Jenjarom Selangor, MALAYSIA

*Corresponding Author: sakhiah@uitm.edu.my

DOI: <https://doi.org/10.30880/ijscet.2024.15.01.021>

Article Info

Received: 27 February 2024

Accepted: 25 March 2024

Available online: 15 July 2024

Keywords

Operational modal analysis, finite element model, ambient vibration test, natural frequency, mode shape

Abstract

The integration of Operational Modal Analysis (OMA) and Finite Element Model (FEM) techniques has proven to be a valuable approach for evaluating and maintaining the health of such structures. OMA extracts dynamic characteristics from a bridge's responses to ambient vibrations, while FEM employs computational models to simulate and compare these dynamic behaviours. This comprehensive methodology ensures an accurate representation of the bridge's behaviour and its correlation with real-world conditions. However, a significant challenge arises in assessing the Ultra High Performance Fiber Reinforced Concrete (UHPFRC) pedestrian bridge in Klang, Selangor, launched in October 2022, due to limited available information about OMA and FEM on UHPFRC. This research aims to develop FEM and conduct ambient vibration tests to obtain modal parameters. Moreover, the study investigates OMA techniques in the context of weak excitation sources, filling a critical knowledge gap. By comparing experimental results with FEM, this research provides insights into the feasibility and reliability of OMA under challenging environmental conditions. The principal results reveal significant percentage differences in natural frequencies between FEM and OMA, with the most notable disparities occurring in the first mode. Nevertheless, the mode shapes extracted from OMA closely resemble those from FEM. In conclusion, this research enhances the understanding of UHPFRC pedestrian bridge behaviour and modal analysis techniques.

1. Introduction

Ultra-High-Performance Fiber-Reinforced Concrete (UHPFRC) is an advanced cement-based material characterized by exceptional strength, ductility, and durability. It exhibits a compressive strength exceeding 150 MPa, making it significantly stronger than conventional concrete research from Habel *et al.*, and Saidin *et al.*, [1,2]. UHPFRC incorporates a dense matrix of fine particles, often with a reduced water-cement ratio, and a high volume of steel or polymer fibers, enhancing its tensile strength and toughness stated by Yoo *et al.*, [3]. This

material is known for its outstanding mechanical properties, making it suitable for various demanding applications in construction and infrastructure. Additionally, UHPFRC has remarkable durability, making it resistant to environmental factors and extending the lifespan of structures. Its versatility and impressive performance characteristics have made UHPFRC a valuable innovation in the field of construction materials, offering solutions for challenging engineering projects and sustainable infrastructure development [4].

Structural Health Monitoring (SHM) encompasses two main approaches, passive SHM and active SHM according to Giurgiutiu, [5]. Passive SHM primarily involves measuring various parameters and responses within a structure to assess its health, with a focus on detecting impacts or fiber breakage in composite materials as defined by Etxaniz *et al.*, [6]. Active SHM, on the other hand, employs techniques that actively induce stress or vibrations into a structure, allowing the detection of various types of defects or abnormalities. Giurgiutiu, [7] specified these methods often rely on sensors permanently placed on structures and monitored over time. Overall, SHM plays a critical role in ensuring the safety and longevity of structures by enabling the early detection of damage or deterioration through passive and active monitoring approaches studied from Ozer & Feng, and Pallarés *et al.*, [8,9].

Meanwhile, Finite Element Model (FEM) is a computational technique used in engineering to analyse and simulate complex physical systems by Girardi *et al.*, [10]. Saidin *et al.*, [11] stated ABAQUS is a widely-used finite element analysis software suite. Natural frequency refers to the inherent vibration frequency at which a structure or system oscillates when subjected to external forces. According to Jewell *et al.*, [12], mode shape on the other hand, describes the spatial pattern of motion associated with a particular natural frequency. These concepts are crucial in structural engineering and mechanical analysis according to Korus *et al.*, and Lisbôa *et al.*, [13,14]. Modal analysis, as demonstrated by Saidin *et al.*, [11], helps determine natural frequencies and mode shapes of systems, aiding in understanding structural behaviour, design optimization, and identifying potential issues like cracks in materials, as showcased by Mia *et al.*, [15].

Ambient vibration testing (AVT) is a non-destructive technique used to assess the dynamic characteristics of structures and materials under natural excitation, such as traffic-induced vibrations, human activities and wind loads as mentioned by Ellobody, [16]. This method involves the measurement and analysis of vibrations occurring in the environment surrounding the structure of interest. AVT are valuable in various engineering applications, including assessing the structural integrity of bridges, historic buildings, and other infrastructure studies from Foti *et al.*, and Saidin *et al.*, [17,11]. Compan *et al.*, [18] stated that by capturing the naturally occurring vibrations, engineers and researchers can determine fundamental properties such as natural frequencies, mode shapes, and damping ratios. These findings as stated by Gentile & Saisi, [19] are essential for SHM, damage assessment, and the development of accurate numerical models for predicting the dynamic behaviour of structures. AVT plays a significant role in ensuring the safety and longevity of critical infrastructure and cultural heritage preservation.

However, there is a lack of specific studies on reinforced concrete pedestrian bridges and their current condition. Limited research has focused on structures with short to moderate span lengths that experience only weak environmental excitation sources Chen *et al.*, [20]. The primary concern in such scenarios lies in the low signal-to-noise ratio (SNR) of collected vibration responses, which makes accurate modal parameter extraction a formidable task. This research aims to assess the structural condition of a UHPFRC pedestrian bridge through Operational Modal Analysis (OMA) and FEM techniques. The ultimate goal is to develop a finite element model and conduct ambient vibration tests to obtain modal parameters.

2. Literature Review or Related Research

This literature review explores bridge engineering, covering various structures, analysis methods, and monitoring techniques. Bridge design includes arch, truss, suspension, cable-stayed, and cantilever bridges, balancing architectural elegance with structural stability. Analysis techniques like FEM and health monitoring methods such as AVT and OMA are crucial for understanding and maintaining bridge integrity. Techniques like Frequency Domain Decomposition (FDD) and Stochastic Subspace Identification (SSI) further enhance analysis capabilities. Despite advancements, bridging theory and practice remains essential for improving bridge engineering and ensuring safety.

2.1 Bridge Structure

A bridge structure consists of several key components, including the deck, joists, piers, and abutments. The deck serves as the roadway surface, supported by joists, while piers provide vertical support. Abutments anchor the bridge ends and distribute loads into the surrounding terrain Wang *et al.*, [21]. In water environments, piles and concrete caissons serve as foundation elements Eslami *et al.*, [22]. Bridge design aims to balance structural integrity, aesthetic appeal, and functionality, with suspension bridges featuring stiffening girders/trusses, main suspension cables, towers, and anchorages Lin & Yoda, [23]. Advanced designs like composite box girders with corrugated steel webs and trusses enhance performance and durability. Aesthetics are crucial in bridge design,

ensuring integration with the environment Chen *et al.*, [24]. Displacement criteria of bridge structures can offer insights into geological phenomena, aiding in understanding processes like fault displacement. Engineers continuously improve practices to address challenges such as disproportionate collapse, prioritizing safety and resilience Derseh & Mohammed, [25].

2.2 Bridge Health Monitoring

Bridge health monitoring is essential for ensuring structural integrity and safety, involving continuous assessment using various techniques Yapar *et al.*, [26]. Recent advancements in SHM utilize wireless sensor networks to collect real-time data on vibrations, strains, and environmental conditions Di Graziano *et al.*, [27]. Non-destructive testing (NDT) methods such as AVT and ultrasound aid in identifying hidden defects and material degradation without causing damage Saidin *et al.*, and Pallarés *et al.*, [11,9]. Integration with technologies like mixed reality and machine learning enhances monitoring capabilities Karaaslan *et al.*, [28].

2.3 Weak Excitation

Weak excitation, a method in bridge health monitoring, involves assessing structural integrity using low-energy stimuli to minimize strain on the bridge Lan *et al.*, and Xin *et al.*, [29,30]. This approach, employing small vibrations below the resonant frequency, detects subtle damage not discernible through conventional methods Ngeljaratan & Moustafa, [31]. It aids in early-stage damage detection and long-term health assessment, contributing to bridge safety Prada *et al.*, and Xue & Psimoulis, [32,33]. Combining advanced algorithms with sensors enables informed decisions on maintenance Gao *et al.*, and Malekjafarian *et al.*, [34,35], continuously evolving for enhanced bridge longevity.

2.4 Modal Identification

Modal identification is crucial for understanding dynamic behavior, involving determining natural frequencies, damping ratios, and mode shapes Han *et al.*, 2023 and Çelebi & Kaya, [36,37]. Techniques include modal tests and operational modal analysis, particularly useful when excitation sources are limited. Algorithms like Fully Automated Operational Modal Identification aid in efficient parameter determination, validating finite element models Mostafaei *et al.*, [38]. Advancements include portable laser-and-camera systems for cost-effective modal identification Han *et al.*, [36] and multi-camera arrays for accurate measurement Zhu *et al.*, [39]. Unified methods address challenges in mode separation and tracking M. He *et al.*, [40], advancing structural analysis.

2.5 Operational Modal Analysis (OMA)

OMA evaluates dynamic behavior based on structural response to ambient excitation. By extracting modal parameters from the structural response, OMA enables the identification of natural frequencies, damping ratios, and mode shapes, which are essential for structural health monitoring Zhou *et al.*, [41]. It validates finite element models, particularly for tall structures, like bridges, wind turbines, and high-rise buildings Avci *et al.*, [42]. Automated procedures handle large datasets from long-term monitoring, aiming to enhance accuracy and reliability Zini *et al.*, [43]. Fully automated approaches, like a three-stage clustering algorithm, eliminate user interaction and subjective decisions Reynders *et al.*, [44]. OMA finds applications in nuclear reactor characterization and optimization, including neutron noise analysis Torres Delgado *et al.*, [45]. Transmissibility-based methods, such as TOMA, offer versatility and independence from excitation spectrum Dario Gómez Araújo, [46]. Comparative studies assess estimation accuracy, proposing novel approaches like order-based methods Sternharz *et al.*, [47]. OMA, combined with mode tracking, studies vibration characteristics of flexible ship structures, aiding structural analysis and fatigue assessment van Zijl *et al.*, [48]. Machine learning approaches automate OMA, eliminating setup requirements and extracting modal parameters efficiently Mugnaini *et al.*, [49].

2.6 Frequency Domain Decomposition (FDD)

FDD estimates natural frequencies and mode shapes using singular value decomposition of Power Spectral Densities (PSDs) obtained from measured vibration responses, gaining popularity for its simplicity and robustness. FDD proves useful in multi-dataset output-only modal analysis, facilitating natural frequency and mode shape identification Amador & Brincker, [50]. Its applications span mechanical and nuclear engineering, structural health monitoring, and system identification, aiding dynamic feature extraction, damage identification, and model updating Tarinejad & Damadipour, Torres Delgado *et al.*, and C. Zhang *et al.*, [51,45,52].

2.7 Stochastic Subspace Identification (SSI)

SSI extracts dynamic system modal parameters from measured response data, valuable for operational modal analysis and power system stability. It enhances decision-making in designing and maintaining structures and systems, offering solid mathematical foundations and efficient results assessment Y. C. He *et al.*, and D. Liu *et al.*, [53, 54] SSI's accuracy in identifying electromechanical modes influences power system stability assessment, with recent extensions incorporating machine learning techniques to improve efficiency and accuracy Arunagirinathan & Venayagamoorthy, and D. Liu *et al.*, [55.54]. Efforts to enhance SSI's efficiency for real-time applications include fast online implementations, retaining accuracy while expediting system identification Sun *et al.*, [56].

3. Methodology

The research methodology for this study comprises several interconnected steps. Initially, a site inspection of the Kapar UHPFRC pedestrian bridge will be conducted, focusing on the collection of pertinent data related to the bridge's geometry, material properties and construction details. Subsequently, utilizing the collected information and identified modal parameters, will proceed to develop a precise FEM of the bridge. This FEM will be generated using Abaqus, a finite element analysis software, and will accurately represent the bridge's geometry and material properties.

In the next phase, AVT will be carried out on the bridge. A vibration sensor will be strategically positioned at multiple locations on the bridge to capture its dynamic response to ambient loads. The data acquired through this testing will then be employed in the identification of the bridge's natural frequencies, mode shapes, and damping ratios, a process facilitated by OMA.

Finally, the modal parameters obtained from the FEM will be compared to the data obtained from the AVT. This comparative analysis will allow us to calculate the percentage difference, which in turn will aid in our assessment of the bridge's structural condition.

The research methodology employed in this study comprises several key steps. First, a FEM of the Kapar UHPFRC pedestrian bridge is developed using Abaqus software, utilizing collected data and identified modal parameters to accurately represent the bridge's geometry as shown in Fig. 1 and material properties in Table 1.

3.1 Finite Element Model (FEM)

A FEM of the Kapar UHPFRC pedestrian bridge has been developed using Abaqus software. This model makes use of collected data from site inspection and identified parameters according to Dura, [57] booklet to precisely represent the bridge's geometry with dimensions, as illustrated in Fig. 1, and material properties as detailed in Table 1.

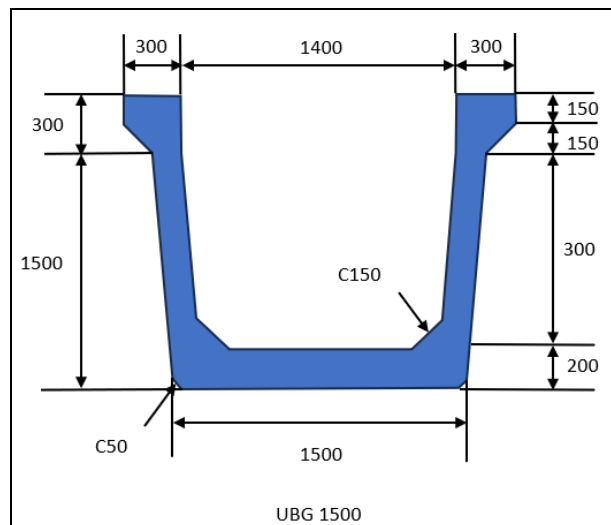


Fig. 1 Cross sectional of DURA UBG1500 UHPFRC (unit length in mm)

Table 1 Material properties of Abaqus bridge model

Components	Modulus of Elasticity (GPa)	Specific Density (kg/m ³)	Poisson's Ratio
Standard	BS EN 12390-13	BS EN 12390-7	BS EN 12390-13
Values	213000 MPa	2400 kg/m ³	0.2

3.2 Ambient Vibration Test

The selected pedestrian bridge in Fig. 2 was constructed in front of SRJK (C) Pui Ying, located on Jalan Kapar (FT005) in Sementa, Klang, Selangor. The project reached completion on October 7, 2022. This bridge is designed as a single-span structure, with approximate dimensions of 39.35 meters in length and 2.5 meters in width. It incorporates a UHPFRC composite pedestrian bridge system. The superstructure of the bridge consists of a single piece of DURA® UBG1500-39.35m, as previously shown in Fig. 1, with a cast-in-situ reinforced concrete (RC) deck. The substructure includes RC columns, and the foundation is supported by 400mm diameter spun piles (Class B). The bridge is engineered to withstand a loading type of 5kPa, in accordance with BD37/01 standards.

**Fig. 2** UHPFRC pedestrian bridge

An ambient vibration test was conducted using accelerometers as shown in Fig. 3 from PCB Piezotronics, strategically positioned at ten different locations along the bridge deck, as illustrated in Fig. 4.

**Fig. 3** Accelerometer sensor

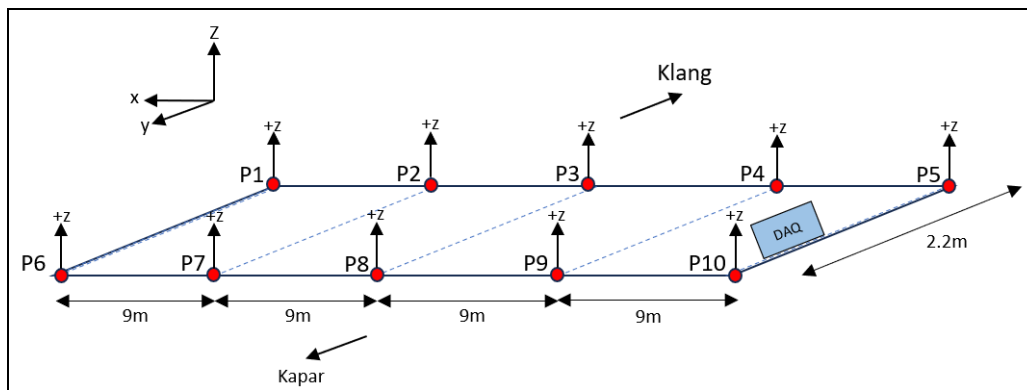


Fig. 4 3D view placement of sensors

Calibration of each sensor was performed to ensure measurement reliability, and data acquisition was facilitated through a DAQ unit connected to a laptop in Fig. 5. The data collected during a 20-minute period of AVT, at a sampling rate of 100Hz, were subsequently processed using ARTeMIS Pro Software 7.0 for operational modal analysis. Additionally, wind speed and temperature data were recorded for further analysis.

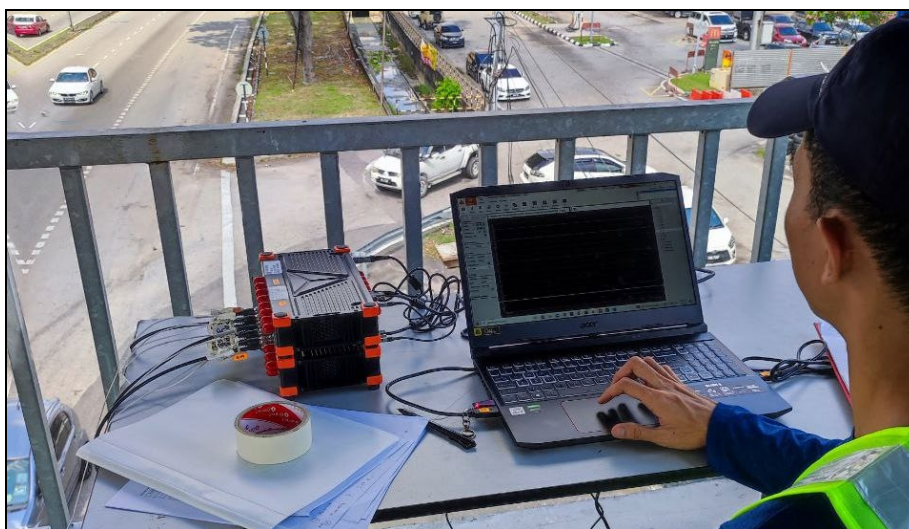


Fig. 5 DAQ connected to laptop

4. Results and Discussion

The results and discussions in this study focus on the natural frequencies and mode shapes obtained through FEM and OMA. The natural frequencies, a critical parameter in structural dynamics, are compared between these two techniques to assess their accuracy and reliability. Additionally, the corresponding mode shapes extracted from FEM and OMA are analysed to understand the similarities and differences in their modal characteristics.

4.1 Natural Frequency

The natural frequencies were obtained through the peak-picking method applied to the OMA outputs from Artemis Modal Pro software shown in the red circle in Fig. 6. Table 2 displays the natural frequencies of a system across five different modes, measured using both the FEM and OMA with various techniques, such as Frequency Domain Decomposition (FDD), Enhanced Frequency Domain Decomposition (EFDD), Complex Frequency Domain Decomposition (CFDD), Stochastic Subspace Identification Unweighted Principal Component (SSI-UPC), Stochastic Subspace Identification Extended Unweighted Principal Component (SSI-UPCX), and Stochastic Subspace Identification Principal Component (SSI-PC).

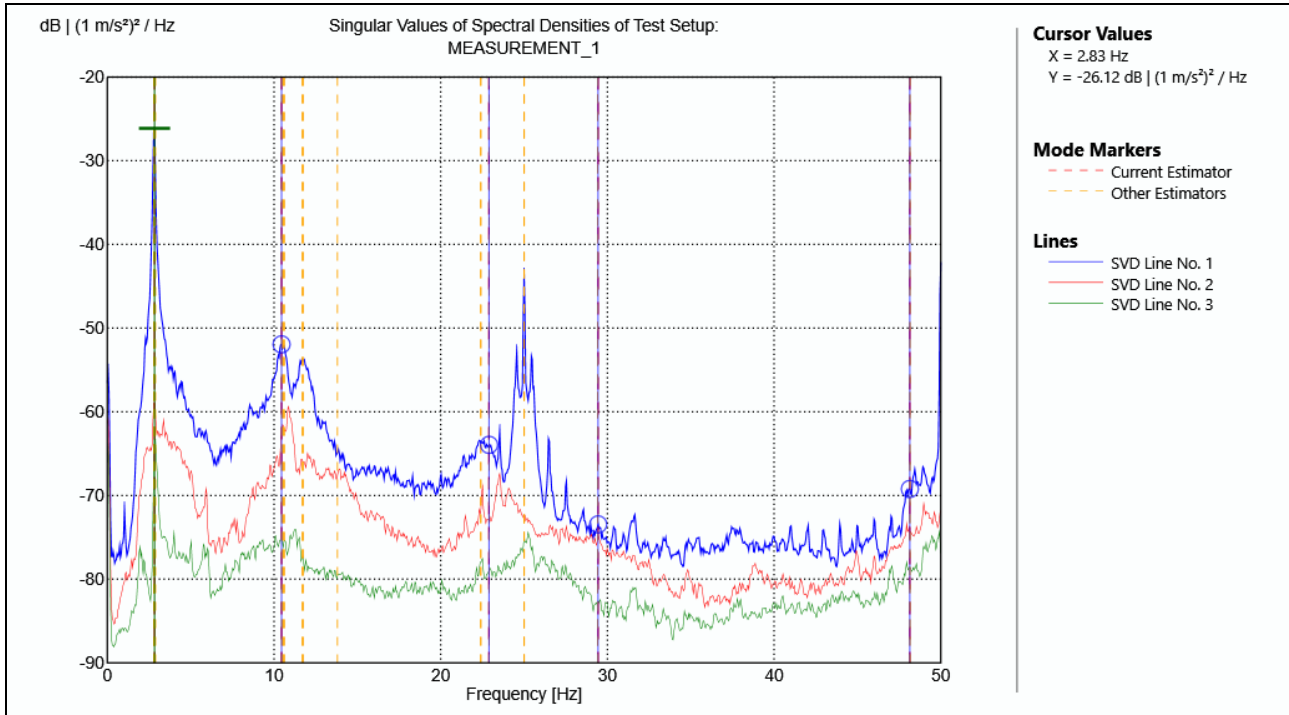


Fig. 6 Natural frequency (OMA) using artemis modal pro

Table 2 Modes and natural frequencies from FEM and OMA

Modes	f _{fem} (Hz)	f _{oma} (Hz)						
		FDD	Complexity	EFDD	CFDD	SSI-UPC	SSI-PC	SSI-UPCX
1	6.9	2.832	0.059	2.807	2.808	2.809	2.808	2.809
2	18.067	10.449	0.667	10.477	10.469	10.549	10.6	10.613
3	33.299	22.9	4.373	22.405	22.409	-	-	22.911
4	30.604	29.443	4.657	29.421	29.421	-	-	-
5	61.304	48.145	3.313	48.145	48.145	-	-	-

The modes 1 to 5 represent the 1st vertical bending, 2nd vertical bending, 3rd vertical bending, 1st torsion, and 2nd torsion, respectively. The natural frequencies for f_{fem} from modes 1 to 5 are 6.9 Hz, 18.067 Hz, 33.299 Hz, 30.604 Hz, and 61.304 Hz. Meanwhile, the natural frequencies for f_{oma} are 2.832 Hz, 10.449 Hz, 22.9 Hz, 29.443 Hz, and 48.145 Hz for modes 1 to 5. The majority of modes from f_{oma} exhibited complexity values of less than 5%. Moreover, all algorithms yielded five natural frequencies. It is noteworthy that SSI-UPC and SSI-PC failed to predict the frequencies of the third to fifth modes, while SSI-UPCX could not predict the frequencies of the fourth and fifth modes.

Statistical analysis involved determining the percentage difference between the natural frequencies obtained from the FEM (f_{fem} in Hz) and those from OMA (f_{oma} in Hz) in FDD by using relative error Eq. [1] from Saidin *et al.*, [11]. Given FDD's straightforward modal extraction via the peak-picking method on its SVD, it was chosen as the benchmark. Such a minimalistic approach allowed for a high degree of certainty in inferring the modes. Table 3 presents the findings, indicating that the most significant percentage difference occurred in the first mode (up to 143.64%), while the lowest discrepancy was observed in the fifth mode (only 3.94%).

$$\Delta f = \frac{f_{oma} - f_{fem}}{f_{oma}} \times 100 \tag{1}$$

Table 3 Percentage difference of natural frequencies between FEM and OMA

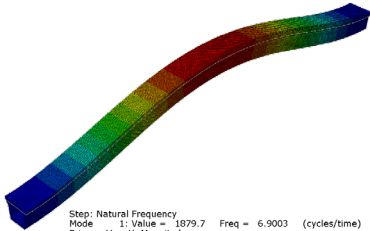
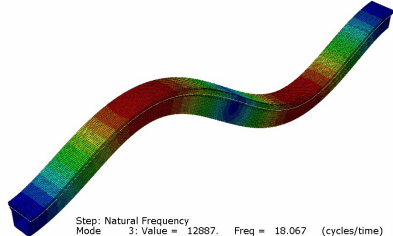
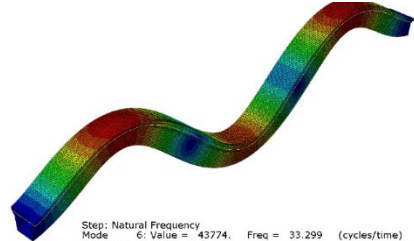
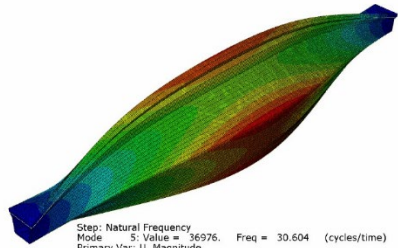
Modes	f _{fem} (Hz)	f _{oma} (Hz)	Percentage Difference (%)
1	6.9	2.832	143.64

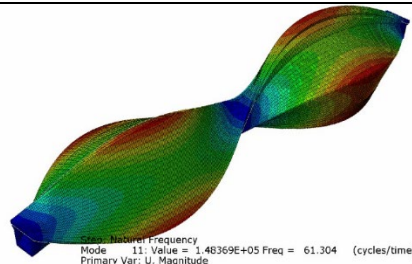
2	18.067	10.449	72.91
3	33.299	22.9	45.41
4	30.604	29.443	3.94
5	61.304	48.145	27.33

4.2 Mode Shape

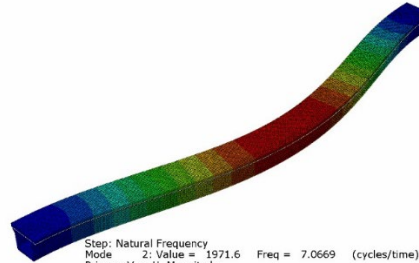
The FEM analysis in this study extracted a total of eight different modes which is first vertical bending, second vertical bending, third vertical bending, first torsion, second torsion, first lateral bending, second lateral bending and third lateral bending. The positions of these modes were also identified in the OMA data. However, the identification process did not yield many distinct modes due to the used of vertical axis accelerometers only. Consequently, the OMA method could only report up to five mode shapes such as first vertical bending, second vertical bending, third vertical bending, first torsion and second torsion. Table 4 illustrates these eight extracted mode shapes along with the natural frequencies obtained from this pedestrian bridge study.

Table 4 Natural frequencies and mode shape of FEM

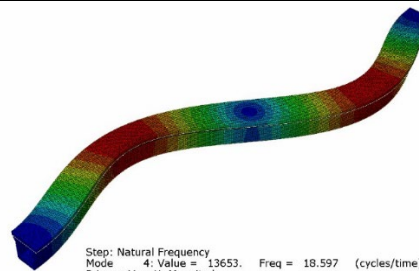
Mode shape	Natural frequency, f
 <p>Step: Natural Frequency Mode 1: Value = 1879.7 Freq = 6.9003 (cycles/time) Primary Var: U, Magnitude</p> <p>1st vertical bending (No. 1)</p>	6.9003
 <p>Step: Natural Frequency Mode 3: Value = 12087. Freq = 18.067 (cycles/time) Primary Var: U, Magnitude</p> <p>2nd vertical bending (No. 2)</p>	18.067
 <p>Step: Natural Frequency Mode 6: Value = 43774. Freq = 33.299 (cycles/time) Primary Var: U, Magnitude</p> <p>3rd vertical bending (No. 3)</p>	33.299
 <p>Step: Natural Frequency Mode 5: Value = 36976. Freq = 30.604 (cycles/time) Primary Var: U, Magnitude</p> <p>1st torsion (No. 4)</p>	30.604



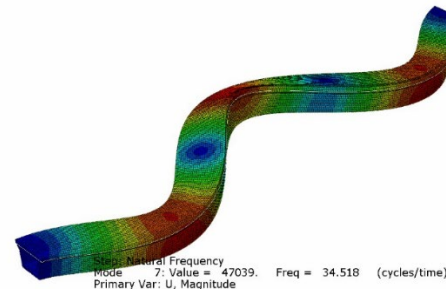
61.304

2nd torsion (No. 5)

7.067

1st lateral bending (No. 6)

18.597

2nd lateral bending (No. 7)

34.518

3rd lateral bending (No. 8)

In Abaqus mode shape analysis, the use of blue and red colour contours serves as a graphical representation to convey information about the behaviour of a structure under different modes of vibration. These colour contours are a valuable tool for engineers and analysts to visually interpret and understand how various points on the structure respond to specific vibrational modes.

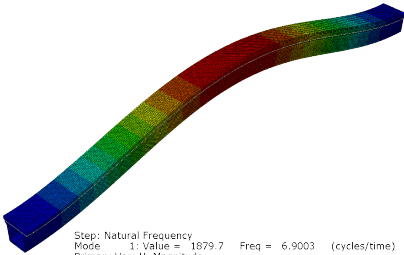
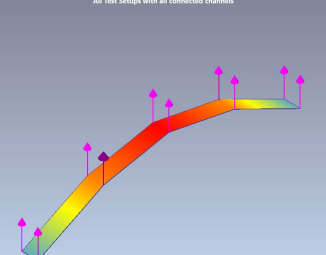
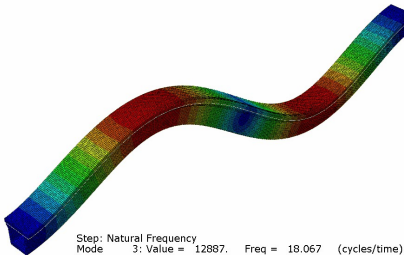
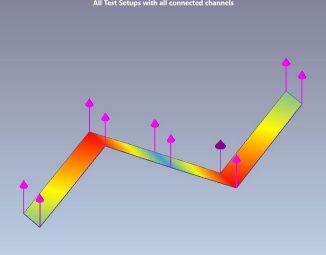
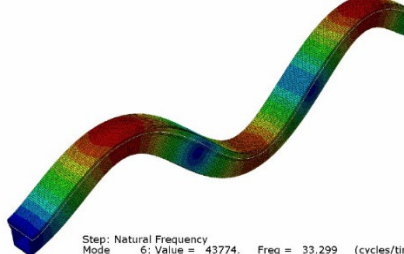
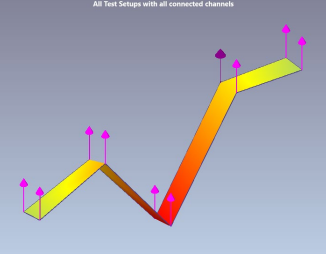
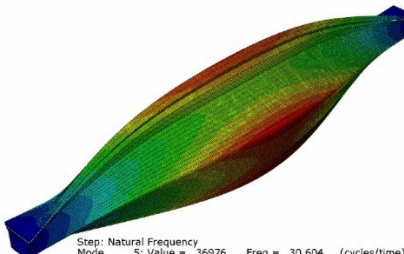
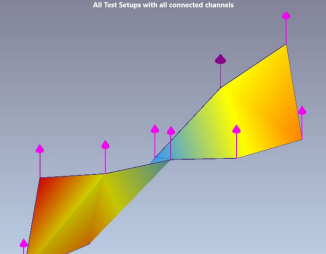
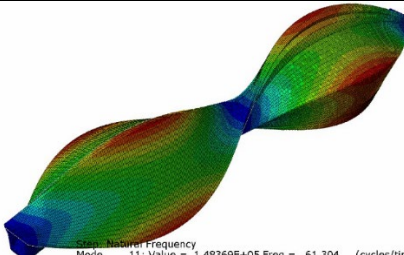
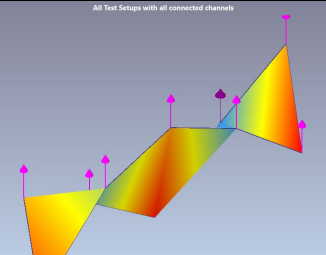
Blue colour contours, typically seen on the plot, signify areas of minimal or no deflection or displacement. In essence, they represent regions of the structure that remain relatively stationary or experience very little deformation when subjected to the analysed mode of vibration. These areas are often referred to as "nodal" points where the displacement is close to zero. Blue contours help pinpoint portions of the structure that remain stable and unaffected by the mode shape being studied.

Conversely, red colour contours are indicative of regions with higher deflection or displacement. When a part of the structure exhibits a red colour, it signifies that this area undergoes significant deformation or movement in response to the specific mode of vibration under consideration. These red areas highlight where the structure is most flexible or experiences the greatest displacement, providing crucial insights into the dynamic behaviour of the structure.

Table 5 highlights the five mode shapes retrieved through OMA and those obtained through FEM. It shows that the mode shape for 1st, 2nd, and 3rd vertical bending is almost the same in FEM and OMA, while the mode shapes for 1st and 2nd torsion are quite different in terms of colour contour. However, to convey these modes more comprehensibly, further validation of their precise magnitudes is necessary, potentially using a greater number of sensors. While experimental work heavily relies on the available data at a specific location, FEM

modes provide precise magnitudes calculated by the Abaqus software. Accurately determining the actual behaviour of mode shapes from experiments can be challenging due to factors such as sensitivity, sensor attachment, and excitation quality. Future research may also consider using Modal Assurance Criterion (MAC) parameters as a useful measurement tool for assessing mode similarity.

Table 5 Mode shape of FEM and OMA

Final Element Model (FEM)	Operational Modal Analysis (OMA)
 <p>Step: Natural Frequency Mode 1: Value = 1579.7 Freq = 6.9003 (cycles/time) Primary Var: U, Magnitude</p> <p>1st vertical bending (No. 1)</p>	 <p>All Test Setups with all connected channels</p>
 <p>Step: Natural Frequency Mode 3: Value = 12887. Freq = 18.067 (cycles/time) Primary Var: U, Magnitude</p> <p>2nd vertical bending (No. 2)</p>	 <p>All Test Setups with all connected channels</p>
 <p>Step: Natural Frequency Mode 6: Value = 43774. Freq = 33.299 (cycles/time) Primary Var: U, Magnitude</p> <p>3rd vertical bending (No. 3)</p>	 <p>All Test Setups with all connected channels</p>
 <p>Step: Natural Frequency Mode 5: Value = 36976. Freq = 30.604 (cycles/time) Primary Var: U, Magnitude</p> <p>1st torsion (No. 4)</p>	 <p>All Test Setups with all connected channels</p>
 <p>Step: Natural Frequency Mode 11: Value = 1.48369E+05 Freq = 61.304 (cycles/time) Primary Var: U, Magnitude</p> <p>2nd torsion (No. 5)</p>	 <p>All Test Setups with all connected channels</p>

5. Conclusions

A pedestrian bridge underwent several modal analysis studies to better understand its structural behaviour. These studies aimed to determine the bridge's natural frequencies, comparing the results obtained through the FEM with experimental computation techniques derived from OMA.

The algorithms employed in these studies successfully identified all of the natural frequencies, aligning closely with those calculated using the FEM method. In addition, during an ambient vibration test of the pedestrian bridge, five distinct mode shapes were extracted for comparison. There are significant percentage differences in natural frequencies between FEM and OMA. Notably, three modes identified in the OMA mode shapes closely resembled those obtained through the FEM method.

To enhance the precision of mode shape extraction in future experiments, it is recommended to conduct further verification using additional accelerometers and lateral axis sensors. Furthermore, it is essential to acknowledge that a significant percentage difference exists between the measured and predicted natural frequencies. Therefore, it is advisable to perform a Finite Element Model Updating (FEMU) to ensure a more accurate match between the measured and predicted modal parameters.

Acknowledgement

The authors would like to express their gratitude to the School of Civil Engineering and College of Engineering, Universiti Teknologi MARA, Shah Alam for supporting this publication via research grant 600-TNCPI 5/3/DDF (KPK) (003/2023).

Conflict of Interest

Authors declare that there is no conflict of interests regarding the publication of the paper.

Author Contribution

The authors confirm contribution to the paper as follows: **study conception and design:** Hussein Muhammad, Sakhiah Abdul Kudus, Adiza Jamadin, Siti Shahirah Saidin; **data collection:** Hussein Muhammad; Sakhiah Abdul Kudus, Adiza Jamadin, Siti Shahirah Saidin; **analysis and interpretation of results:** Hussein Muhammad, Sakhiah Abdul Kudus, Adiza Jamadin, Siti Shahirah Saidin; **draft manuscript preparation:** Hussein Muhammad, Sakhiah Abdul Kudus. All authors reviewed the results and approved the final version of the manuscript.

References

- [1] Habel, K., Viviani, M., Denarié, E., & Brühwiler, E. (2006) Development of the mechanical properties of an Ultra-High Performance Fiber Reinforced Concrete (UHPFRC). *Cement and Concrete Research*, 36(7), 1362–1370, <https://doi.org/10.1016/J.CEMCONRES.2006.03.009>
- [2] Saidin, S. S., Kudus, S. A., Jamadin, A., Anuar, M. A., Amin, N. M., Ya, A. B. Z., & Sugiura, K. (2023) Vibration-based approach for structural health monitoring of ultra-high-performance concrete bridge. *Case Studies in Construction Materials*, 18, <https://doi.org/10.1016/j.cscm.2022.e01752>
- [3] Yoo, D. Y., Shin, H. O., Yang, J. M., & Yoon, Y. S. (2014) Material and bond properties of ultra high performance fiber reinforced concrete with micro steel fibers. *Composites Part B: Engineering*, 58, 122–133, <https://doi.org/10.1016/J.COMPOSITESB.2013.10.081>
- [4] Akeed, M. H., Qaidi, S., Ahmed, H. U., Faraj, R. H., Mohammed, A. S., Emad, W., Tayeh, B. A., & Azevedo, A. R. G. (2022) Ultra-high-performance fiber-reinforced concrete. Part IV: Durability properties, cost assessment, applications, and challenges. *Case Studies in Construction Materials*, 17, e01271, <https://doi.org/10.1016/J.CSCM.2022.E01271>
- [5] Giurgiutiu, V. (2014) *Structural Health Monitoring with Piezoelectric Wafer Active Sensors*. Academic Press. <https://doi.org/10.1016/B978-0-12-418691-0.00001-0>
- [6] Etxaniz, J., Aranguren, G., Gil-García, J. M., Sánchez, J., Vivas, G., & González, J. (2023) Ultrasound-based structural health monitoring methodology employing active and passive techniques. *Engineering Failure Analysis*, 146, 107077. <https://doi.org/10.1016/J.ENGFILANAL.2023.107077>
- [7] Giurgiutiu, V. (2015) Structural health monitoring (SHM) of aerospace composites. In P.E. Irving & C. Soutis (Eds.), *Polymer Composites in the Aerospace Industry* (pp. 449–507). Woodhead Publishing. <https://doi.org/10.1016/B978-0-85709-523-7.00016-5>
- [8] Ozer, E., & Feng, M. Q. (2020) Structural health monitoring. In Fernando Pacheco-Torgal, Erik Rasmussen, Claes-Goran Granqvist, Volodymyr Ivanov, Arturas Kaklauskas & Stephen Makonin (Eds.), *Start-Up Creation (Second Edition): The Smart Eco-Efficient Built Environment* (pp. 345–367). Woodhead Publishing. <https://doi.org/10.1016/B978-0-12-819946-6.00013-8>

- [9] Pallarés, F. J., Betti, M., Bartoli, G., & Pallarés, L. (2021) Structural health monitoring (SHM) and Nondestructive testing (NDT) of slender masonry structures: A practical review. *Construction and Building Materials*, 297, 123768, <https://doi.org/10.1016/j.CONBUILDMAT.2021.123768>
- [10] Girardi, M., Padovani, C., Pellegrini, D., Porcelli, M., & Robol, L. (2020) Finite element model updating for structural applications, *Journal of Computational and Applied Mathematics*, 370, 112675, <https://doi.org/10.1016/j.cam.2019.112675>
- [11] Saidin, S. S., Kudus, S. A., Jamadin, A., Anuar, M. A., Amin, N. M., Ibrahim, Z., Zakaria, A. B., & Sugiura, K. (2022) Operational modal analysis and finite element model updating of ultra-high-performance concrete bridge based on ambient vibration test, *Case Studies in Construction Materials*, 16, e01117, <https://doi.org/10.1016/j.cscm.2022.e01117>
- [12] Jewell, E., Allen, M. S., Zare, I., & Wall, M. (2020) Application of quasi-static modal analysis to a finite element model and experimental correlation, *Journal of Sound and Vibration*, 479, 115376, <https://doi.org/10.1016/j.jsv.2020.115376>
- [13] Korus, K., Salamak, M., & Jasiński, M. (2021) Optimization of geometric parameters of arch bridges using visual programming FEM components and genetic algorithm, *Engineering Structures*, 241, 112465, <https://doi.org/10.1016/j.ENGSTRUCT.2021.112465>
- [14] Lisbôa, T. V., Almeida, J. H. S., Spickenheuer, A., Stommel, M., Amico, S. C., & Marczak, R. J. (2022) FEM updating for damage modeling of composite cylinders under radial compression considering the winding pattern, *Thin-Walled Structures*, 173, 108954, <https://doi.org/10.1016/j.tws.2022.108954>
- [15] Mia, M. S., Islam, M. S., & Ghosh, U. (2017) Modal Analysis of Cracked Cantilever Beam by Finite Element Simulation, *Procedia Engineering*, 194, 509–516, <https://doi.org/10.1016/j.PROENG.2017.08.178>
- [16] Ellobody, E. (2023). *Finite Element Analysis and Design of Steel and Steel-Concrete Composite Bridges (Second Edition)*. Butterworth-Heinemann. <https://doi.org/10.1016/C2022-0-00630-9>
- [17] Foti, D., Diaferio, M., Giannoccaro, N. I., & Mongelli, M. (2012) Ambient vibration testing, dynamic identification and model updating of a historic tower, *NDT and E International*, 47, 88-95, <https://doi.org/10.1016/j.ndteint.2011.11.009>
- [18] Compan, V., Pachón, P., & Cámara, M. (2017) Ambient vibration testing and dynamic identification of a historical building. Basilica of the Fourteen Holy Helpers (Germany), *Procedia Engineering*, 199, 3392–3397, <https://doi.org/10.1016/j.proeng.2017.09.572>
- [19] Gentile, C., & Saisi, A. (2007) Ambient vibration testing of historic masonry towers for structural identification and damage assessment, *Construction and Building Materials*, 21(6), 1311-1321, <https://doi.org/10.1016/j.conbuildmat.2006.01.007>
- [20] Chen, G. W., Omenzetter, P., & Beskhyroun, S. (2017) Operational modal analysis of an eleven-span concrete bridge subjected to weak ambient excitations, *Engineering Structures*, 151, 839–860, <https://doi.org/10.1016/j.engstruct.2017.08.066>
- [21] Wang, S., Hagan, P. C., & Cao, C. (2016). Mining Geomechanics. *Advances in Rock-Support and Geotechnical Engineering*, 335–402. <https://doi.org/10.1016/B978-0-12-810552-8.00006-4>
- [22] Eslami, A., Moshfeghi, S., MolaAbasi, H., & Eslami, M. M. (2020). CPT & CPTu for ground modification. *Piezoelectric and Cone Penetration Test (CPTu and CPT) Applications in Foundation Engineering*, 263–297. <https://doi.org/10.1016/B978-0-08-102766-0.00009-2>
- [23] Lin, W., & Yoda, T. (2017). Introduction of Bridge Engineering. *Bridge Engineering*, 1–30. <https://doi.org/10.1016/B978-0-12-804432-2.00001-3>
- [24] Chen, Y., Dong, J., & Xu, T. (2018). Composite box girder with corrugated steel webs and trusses – A new type of bridge structure. *Engineering Structures*, 166, 354–362. <https://doi.org/10.1016/j.ENGSTRUCT.2018.03.047>
- [25] Derseh, S. A., & Mohammed, T. A. (2023). Bridge structures under progressive collapse: A comprehensive state-of-the-art review. *Results in Engineering*, 18, 101090. <https://doi.org/10.1016/j.RINENG.2023.101090>
- [26] Yapar, O., Basu, P. K., Volgyesi, P., & Ledeczki, A. (2015). Structural health monitoring of bridges with piezoelectric AE sensors. *Engineering Failure Analysis*, 56, 150–169. <https://doi.org/10.1016/j.ENGFAILANAL.2015.03.009>
- [27] Di Graziano, A., Marchetta, V., & Cafiso, S. (2020). Structural health monitoring of asphalt pavements using smart sensor networks: A comprehensive review. *Journal of Traffic and Transportation Engineering (English Edition)*, 7(5), 639–651. <https://doi.org/10.1016/j.JTTE.2020.08.001>
- [28] Karaaslan, E., Zakaria, M., & Catbas, F. N. (2022). Mixed reality-assisted smart bridge inspection for future smart cities. *The Rise of Smart Cities: Advanced Structural Sensing and Monitoring Systems*, 261–280. <https://doi.org/10.1016/B978-0-12-817784-6.00002-3>

- [29] Lan, Y., Zhang, Y., & Lin, W. (2023). Diagnosis algorithms for indirect bridge health monitoring via an optimized AdaBoost-linear SVM. *Engineering Structures*, 275, 115239. <https://doi.org/10.1016/j.engstruct.2022.115239>
- [30] Xin, J., Zhou, C., Jiang, Y., Tang, Q., Yang, X., & Zhou, J. (2023). A signal recovery method for bridge monitoring system using TVFEMD and encoder-decoder aided LSTM. *Measurement*, 214, 112797. <https://doi.org/10.1016/j.measurement.2023.112797>
- [31] Ngeljaratan, L., & Moustafa, M. A. (2020). Structural health monitoring and seismic response assessment of bridge structures using target-tracking digital image correlation. *Engineering Structures*, 213, 110551. <https://doi.org/10.1016/j.engstruct.2020.110551>
- [32] Prada, M. A., Toivola, J., Kullaa, J., & Hollmén, J. (2012). Three-way analysis of structural health monitoring data. *Neurocomputing*, 80, 119–128. <https://doi.org/10.1016/j.neucom.2011.07.030>
- [33] Xue, C., & Psimoulis, P. A. (2023). Monitoring the dynamic response of a pedestrian bridge by using low-cost GNSS receivers. *Engineering Structures*, 284, 115993. <https://doi.org/10.1016/j.engstruct.2023.115993>
- [34] Gao, S., Zhao, W., Wan, C., Jiang, H., Ding, Y., & Xue, S. (2022). Missing data imputation framework for bridge structural health monitoring based on slim generative adversarial networks. *Measurement*, 204, 112095. <https://doi.org/10.1016/j.measurement.2022.112095>
- [35] Malekjafarian, A., Corbally, R., & Gong, W. (2022). A review of mobile sensing of bridges using moving vehicles: Progress to date, challenges and future trends. *Structures*, 44, 1466–1489. <https://doi.org/10.1016/j.istruc.2022.08.075>
- [36] Han, Y., Wu, G., & Feng, D. (2023). Structural modal identification using a portable laser-and-camera measurement system. *Measurement*, 214, 112768. <https://doi.org/10.1016/j.measurement.2023.112768>
- [37] Çelebi, M., & Kaya, Y. (2022). Seismic monitoring solutions for buildings. *Sensor Technologies for Civil Infrastructures: Volume 2: Applications in Structural Health Monitoring*, 63–101. <https://doi.org/10.1016/B978-0-08-102706-6.00004-0>
- [38] Mostafaei, H., Ghamami, M., & Aghabozorgi, P. (2021). Modal identification of concrete arch dam by fully automated operational modal identification. *Structures*, 32, 228–236. <https://doi.org/10.1016/j.istruc.2021.03.028>
- [39] Zhu, R., Jiang, D., Huang, Z., Xie, L., Zhang, D., & Fei, Q. (2023). Full-field modal identification using reliability-guided frequency-domain-based digital image correlation method based on multi-camera system. *Measurement*, 211, 112567. <https://doi.org/10.1016/j.measurement.2023.112567>
- [40] He, M., Liang, P., Zhang, Y., Yang, F., & Liu, J. xian. (2022). Unified method for fully automated modal identification and tracking with consideration of sensor deployment. *Engineering Structures*, 260, 114223.
- [41] Zhou, J., Kato, B., & Wang, Y. (2023). Operational modal analysis with compressed measurements based on prior information. *Measurement*, 211, 112644. <https://doi.org/10.1016/j.measurement.2023.112644>
- [42] Avci, O., Alkhamis, K., Abdeljaber, O., Alsharo, A., & Hussein, M. (2022). Operational modal analysis and finite element model updating of a 230 m tall tower. *Structures*, 37, 154–167. <https://doi.org/10.1016/j.istruc.2021.12.078>
- [43] Zini, G., Betti, M., & Bartoli, G. (2022). A quality-based automated procedure for operational modal analysis. *Mechanical Systems and Signal Processing*, 164, 108173. <https://doi.org/10.1016/j.ymsp.2021.108173>
- [44] Reynders, E., Houbrechts, J., & De Roeck, G. (2012). Fully automated (operational) modal analysis. *Mechanical Systems and Signal Processing*, 29, 228–250. <https://doi.org/10.1016/j.ymsp.2012.01.007>
- [45] Torres Delgado, L. A., Verma, V., Montalvo, C., Dokhane, A., & García-Berrocal, A. (2021). Operational modal analysis for characterization of mechanical and thermal-hydraulic fluctuations in simulated neutron noise. *Nuclear Engineering and Design*, 373. <https://doi.org/10.1016/j.nucengdes.2020.111017>
- [46] Dario Gómez Araújo, I. (2022). Transmissibility-based operational modal analysis: Unified concept and its application. *Mechanical Systems and Signal Processing*, 178. <https://doi.org/10.1016/j.ymsp.2022.109302>
- [47] Sternharz, G., Kalganova, T., Mares, C., & Meyeringh, M. (2022). Comparative performance assessment of methods for operational modal analysis during transient order excitation. *Mechanical Systems and Signal Processing*, 169. <https://doi.org/10.1016/j.ymsp.2021.108719>
- [48] van Zijl, C., Soal, K., Volkmar, R., Govers, Y., Böswald, M., & Bekker, A. (2021). The use of operational modal analysis and mode tracking for insight into polar vessel operations. *Marine Structures*, 79. <https://doi.org/10.1016/j.marstruc.2021.103043>
- [49] Mugnaini, V., Zanotti Fragonara, L., & Civera, M. (2022). A machine learning approach for automatic operational modal analysis. *Mechanical Systems and Signal Processing*, 170. <https://doi.org/10.1016/j.ymsp.2022.108813>
- [50] Amador, S. D. R., & Brincker, R. (2021). Robust multi-dataset identification with frequency domain decomposition. *Journal of Sound and Vibration*, 508. <https://doi.org/10.1016/j.jsv.2021.116207>

- [51] Tarinejad, R., & Damadipour, M. (2014). Modal identification of structures by a novel approach based on FDD-wavelet method. *Journal of Sound and Vibration*, 333(3), 1024–1045. <https://doi.org/10.1016/j.jsv.2013.09.038>
- [52] Zhang, C., Mousavi, A. A., Masri, S. F., Gholipour, G., Yan, K., & Li, X. (2022). Vibration feature extraction using signal processing techniques for structural health monitoring: A review. In *Mechanical Systems and Signal Processing* (Vol. 177). Academic Press. <https://doi.org/10.1016/j.ymssp.2022.109175>
- [53] He, Y. C., Li, Z., Fu, J. Y., Wu, J. R., & Ng, C. T. (2021). Enhancing the performance of stochastic subspace identification method via energy-oriented categorization of modal components. *Engineering Structures*, 233, 111917. <https://doi.org/10.1016/j.ENGSTRUCT.2021.111917>
- [54] Liu, D., Bao, Y., & Li, H. (2023). Machine learning-based stochastic subspace identification method for structural modal parameters. *Engineering Structures*, 274, 115178. <https://doi.org/10.1016/j.ENGSTRUCT.2022.115178>
- [55] Arunagirinathan, P., & Venayagamoorthy, G. K. (2018). Effects of Data Size on Stochastic Subspace Identification Method for Power System Electromechanical Modes. *IFAC-PapersOnLine*, 51(13), 668–673. <https://doi.org/10.1016/j.IFACOL.2018.07.357>
- [56] Sun, S., Yang, B., Zhang, Q., Wüchner, R., Pan, L., & Zhu, H. (2023). Fast online implementation of covariance-driven stochastic subspace identification. *Mechanical Systems and Signal Processing*, 197, 110326. <https://doi.org/10.1016/j.YMSSP.2023.110326>
- [57] DURA (2023). DURA Booklet – 5th Edition, Page 44.